Available online at www.sciencedirect.com
SCIENCE DIRECT®
Bioorganic & Medicinal Chemistry Letters
Bioorganic & Medicinal Chemistry Letters 16 (2006) 2543–2548

4-Amino derivatives of the Hsp90 inhibitor CCT018159

Xavier Barril,[a] Mandy C. Beswick,[a] Adam Collier,[a] Martin J. Drysdale,[a,*] Brian W. Dymock,[a] Alexandra Fink,[a] Kate Grant,[a] Robert Howes,[a] Allan M. Jordan,[a] Andrew Massey,[a] Allan Surgenor,[a] Joanne Wayne,[a] Paul Workman[b] and Lisa Wright[a]

[a]*Vernalis Ltd, Granta Park, Cambridge CB1 6GB, UK*
[b]*Cancer Research UK Centre for Cancer Therapeutics, The Institute of Cancer Research, 15 Cotswold Road, Sutton, Surrey SM2 5NG, UK*

Received 5 January 2006; revised 18 January 2006; accepted 18 January 2006
Available online 9 February 2006

Abstract—Novel piperazinyl, morpholino and piperidyl derivatives of the pyrazole-based Hsp90 inhibitor CCT018159 are described. Structure–activity relationships have been elucidated by X-ray co-crystal analysis of the new compounds bound to the N-terminal domain of human Hsp90. Key features of the binding mode are essentially identical to the recently reported potent analogue VER-49009. The most potent of the new compounds has a methylsulfonylbenzyl substituent appended to the piperazine nitrogen, possesses an IC_{50} of less than 600 nM binding against the enzyme and demonstrates low micromolar inhibition of tumour cell proliferation.
© 2006 Elsevier Ltd. All rights reserved.

Exposure of cells to stress, such as heat shock or oxidative stress, results in the accumulation of molecular chaperones, commonly known as heat shock proteins (Hsps). Hsp90 has emerged over the last few years as being of particular interest because of its role in the evolution, development and disease pathology of cancer.[1,2] Hsp90 is an ATP-dependent chaperone essential for the maturation and activity of a varied group of proteins involved in signal transduction, cell cycle regulation and apoptosis.[3,4] Although weak, the ATPase activity can be measured and is selectively inhibited by the ansamycin natural product geldanamycin and its synthetic derivatives 17-AAG and 17-DMAG (Fig. 1).[5,6] In vivo and clinical data with 17-AAG support the hypothesis that the Hsp90 family may be an appropriate target for anti-cancer drug development.[7–9] The chaperone has therefore been the focus of several recent investigations[10] and amongst these, aryl pyrazoles have been reported in the literature as potent small molecule inhibitors.[11]

Our own efforts in this area revealed the 3,4-diaryl pyrazole CCT018159 (**1**), a small molecule inhibitor of Hsp90 ATPase activity.[12] Subsequently, discoveries were made in this series which led to VER-49009.[13] This potent compound was found to display useful levels of inhibition of tumour cell proliferation.

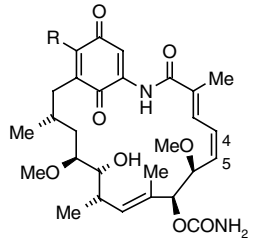

Figure 1. Ansamycin natural product Hsp90 inhibitors.

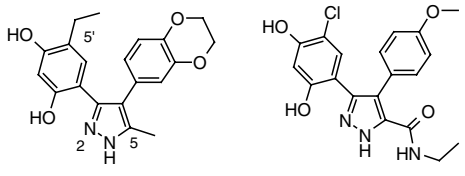

Keywords: Hsp90; Cancer; Structure-based drug design; Pyrazole; X-ray crystallography.
* Corresponding author. Tel.: +44 1223 895555; fax: +44 1223 895556; e-mail: m.drysdale@vernalis.com

0960-894X/$ - see front matter © 2006 Elsevier Ltd. All rights reserved.
doi:10.1016/j.bmcl.2006.01.099

Herein, we describe further developments in this area, revealing a novel series of 3-aryl, 4-aminopyrazoles and characterisation of their binding mode by X-ray co-crystallography.

Optimisation of the screening hit **1** initially focused on improving potency and identifying areas for the introduction of groups to enhance solubility, through the use of the co-crystal structure of **1** and its analogues bound to Hsp90.[12–15] The pyrazole 4-position bearing the 1,4-benzodioxane does not appear to make important interactions with protein.

We have previously shown that the *para*-position of this phenyl ring may be substituted with a large fluorescent group to provide a useful assay probe.[15] Therefore, we surmised that a solubilising group could be placed at the 4-position of the pyrazole ring with minimal impact on potency. Considering requirements for potency, novelty and synthetic access, we determined through modelling studies that cyclic amines were desirable targets.

Indeed when the novel piperazine **2** was prepared, we were delighted to find that ATPase enzyme activity was maintained with only a small loss in growth inhibition against HCT116 colon tumour cells. Binding activity in the FP assay[15] was reduced by nearly 10-fold but this did not affect the functional (ATPase) activity.

From the co-crystal structure of **2** (Fig. 2), key interactions between the resorcinol and the Asp93-water network at the base of the pocket are identical to those observed for **1**.[12–14] Pleasingly, the new piperazine group 4′N overlays closely with the 4′C of the aryl of **1** with no effect on the conformation of the resorcinol–pyrazole system.

This 4′N is clearly important since morpholine **3** looses nearly an order of magnitude of potency. The presence of an acid centre in the vicinity of this position (Asp54) may explain the preference for basic groups.

Alkylation with small lipophiles (**4** and **5**) does not alter potency but further exploration, particularly with benzyl systems, such as **7** and methylsulfonylbenzyl **6**, resulted in significant potency gains of nearly 10-fold.

An inspection of the X-ray co-crystal of **6** bound to Hsp90 reveals that the sulfone moiety makes a direct hydrogen bond with Ser50 (Fig. 3). Furthermore, the steric bulk of the benzylic group forces Asp54 to change its conformation, bringing it closer to the 4′N atom of **6**, thus inducing the formation of a salt bridge. Gratifyingly, cellular potency had also improved.

Increasing the spacer length between the piperazine and phenyl rings results in loss of potency (**8**), as does exchanging the phenyl for an amide (**9**). Alkylation of the pyrazole nitrogen (either isomer) abolished activity due to clash with the residues forming the binding site (Gly97, Thr184 and an interstitial water molecule).[17,18]

In the quest for further potency, we focused on the 5′-position of the resorcinol ring. Ethyl and chloro groups have been reported in the 3,4-diaryl pyrazole series to enhance potency over hydrogen.[12,13] Development of this position by extension into a lipophilic pocket was achieved from bromo **10**, which itself had a similar profile to **2**. This lipophilic pocket does not exist in the native conformation of Hsp90, but we found that it appeared as a result of a conformational change induced by the binding of PU3.[17] Phenethyl **11** induced the same conformational change and bound slightly better to the enzyme but had similar ATPase inhibition.

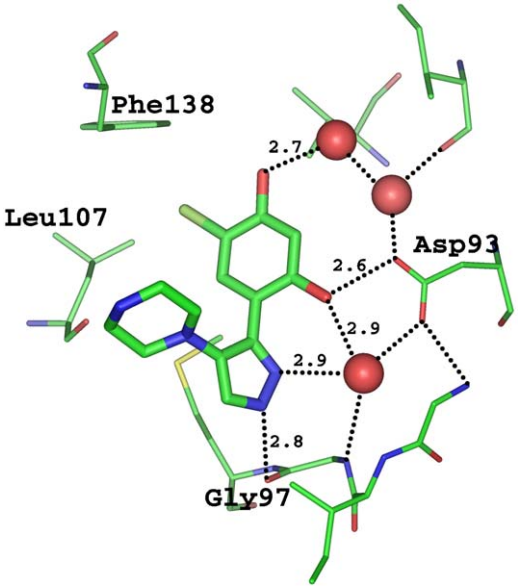

Figure 2. Binding mode of **2** to Hsp90.[21] The dotted lines indicate polar interactions between the ligand, the protein and interstitial water molecules.

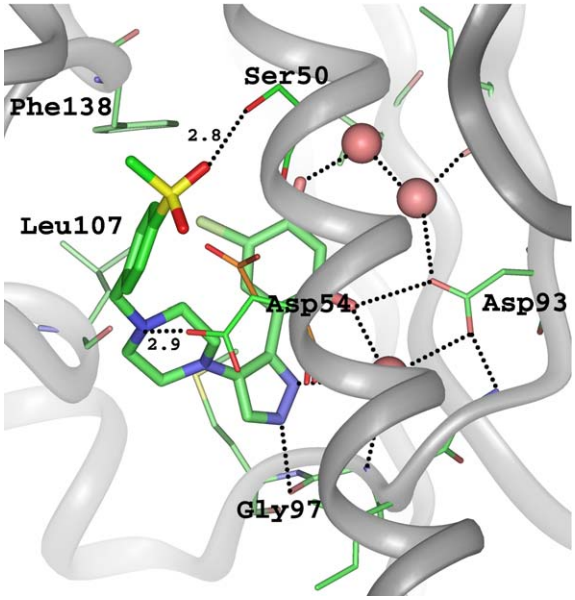

Figure 3. Binding mode of **6** to Hsp90.[21] The conformation of Asp54 in the Hsp90–**2** complex is provided for comparison (orange residue).

Deletion of the ethyl linker to give phenyl **12** had no effect on ATPase or cell activity. These results led to combinations of R^1 and R^2 (where X = N, see Table 1). Alkylating the bromo compound **10** with the sulfonylbenzyl group from **6** gave **13**, which was 10-fold more active than **10** as expected. However, when **11** was similarly treated, the resulting **14** was less active than either **11** or **6**. Clearly these groups are influencing each other. We believe that these aromatic rings stack against each other, forming a conformation incompatible with binding to Hsp90. The loss of activity could then be explained on the basis of an internal energy penalty.

Attention then turned to the 5-position of the pyrazole. As previously reported, an ethyl amide improves potency by at least an order of magnitude in the 3,4-diaryl series.[13] In the piperazine series, however, such SAR is not seen. Methyl **15** was similar to **2** and hydroxyl methyl **16** greater than 10-fold less potent. Unfortunately, ethyl amide **17** was no better or worse than **2**. Overlay of the co-crystal structure of **17** with the structure of **2** bound to Hsp90 shows the binding modes to be virtually identical (Fig. 4). The new amide in **17** even makes the desired hydrogen bond with Gly97.

This disappointing result is explained by the fact that, unlike the analogous 4-phenyl compounds, the conformation observed in the co-crystal structure does not correspond to a global minimum in aqueous solution.

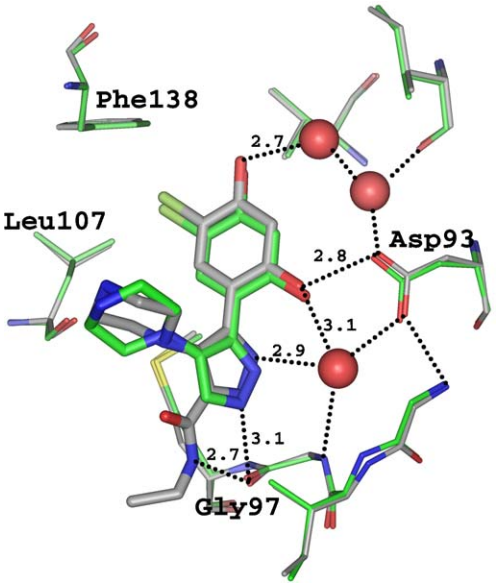

Figure 4. Overlay of X-ray structures of **17** (grey) and **2** (green) bound to Hsp90.[21]

As can be seen in Table 2, compounds such as **17** have to pay a significant internal energy penalty to be able to bind to Hsp90, either in their neutral (2.4 kcal/mol) or protonated form (0.4 kcal/mol). The preference for the *syn* conformation is due to the formation of an inter-

Table 1. Hsp90 inhibitors and their activity[16]

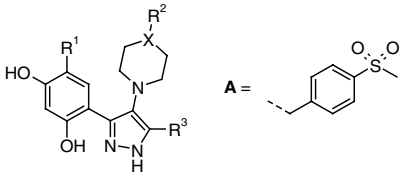

Compound	R^1	XR^2	R^3	FP IC_{50}[a] (μM)	ATPase IC_{50}[b] (μM)	HCT116 GI_{50} (μM)
17-AAG				1.54 (0.5)	17.7 (7.7)	0.17 (0.07)
1				0.148 (0.016)	6.3 (2.9)	5.8 (1.2)
2	Cl	NH	H	2.0 (0.76)	8.2 (2.6)	23.4 (4.8)
3	Cl	O	H	21.7 (3.3)	68.7 (3.0)	>80
4	Cl	NMe	H	8.8 (4.2)	n/d	>80
5	Cl	NEt	H	4.3 (1.8)	11.7 (5.0)	13.8 (4.6)
6	Cl	N-**A**	H	0.74 (0.2)	1.3 (0.4)	3.1 (0.63)
7	Cl	NBn	H	0.6 (0.2)	2.5 (2.3)	6.5 (1.7)
8	Cl	$N(CH_2)_2Ph$	H	4.4 (0.42)	15.5 (2.1)	14.1 (1.6)
9	Cl	NCH_2CONH_2	H	32.6 (14.4)	101 (92)	>80
10	Br	NH	H	9.7 (0.0)	n/d	69.9 (5.2)
11	$PhCH_2CH_2$	NH	H	2.4 (1.6)	9.6 (0.3)	31.6 (4.5)
12	Ph	NH	H	8.5 (3.4)	9.6 (2.5)	>80
13	Br	N-**A**	H	0.6 (0.2)	3.0 (1.7)	8.1 (1.9)
14	$PhCH_2CH_2$	N-**A**	H	5.2 (2.7)	31.8 (7.6)	7.9 (0.9)
15	Cl	NH	Me	3.0 (0.25)	28.3 (2.8)	29.9 (0.3)
16	Cl	NH	CH_2OH	25.1 (4.1)	121.7 (20)	>80
17	Cl	NH	CONHEt	9.5 (0.1)	6.3 (1.2)	34.4 (3.5)
18	Br	CHOH	H	21.2 (8.9)	96.9 (19.6)	>80
19	Br	CHNH-**A**	H	13.9 (2.6)	40.3 (11.6)	73.2 (6.0)
20	Br	CHNHEt	H	5.6 (0.1)	26.1 (5.3)	54.4 (5.2)

FP, fluorescence polarization; all results shown with their standard deviation from at least 2 determinations. n/d, not determined.
[a] IC_{50}'s are obtained from 22 different inhibitor concentrations, Z′ typically >0.9.
[b] IC_{50} determined from 10 different inhibitor concentrations at 2-fold dilutions, Z′ typically >0.75.

Table 2. Relative QM energies (in kcal/mol) of 5-amide pyrazoles in aqueous solution (italics) and in vacuo (parentheses)

Compound	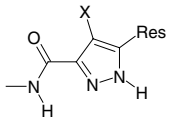	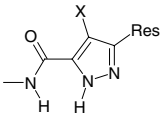	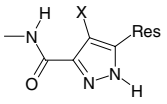	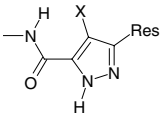
X = 	*0.0* (0.0)	*5.5* (8.9)	*2.1* (4.4)	*2.7* (1.4)
X = 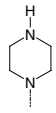	*2.4* (2.6)	*6.4* (8.6)	*0.1* (5.1)	*0.0* (0.0)
X = 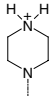	*0.4* (0.0)	*4.7* (11.4)	*0.1* (0.0)	*0.0* (15.1)

The first two columns correspond to the *anti* conformation observed in the X-ray structures. The two rightmost columns correspond to the *syn* conformation, which is incompatible with formation of a hydrogen bond with Gly97. Res, resorcinol.

nal hydrogen bond between NH of the 5-amide and N1 of the piperazine. The fact that, for this type of molecule, both tautomers are isoenergetic may also have an impact on the binding affinity.

Piperidine analogues **18**–**20** were all less potent than the corresponding piperazines.

Piperazine **2** was prepared from commercially available chloro resorcinol. Friedel–Crafts acylation and *O*-benzyl protection of the hydroxyls, followed by bromination of the acyl group, gave key bromomethyl ketone intermediate in moderate overall yield (Scheme 1). Displacement of the bromide was carried out with a range of amine nucleophiles, such as morpholine, which ultimately gives **3**, or protected piperazine (Step d). Homologation with DMF dimethylacetal gives an enamine intermediate which can be cyclised with hydrazine in ethanol in one pot, giving the skeleton of the target molecule. Total deprotection may be accomplished with boron trichloride in DCM to give **2** in 52% yield. Substitution of the piperazine nitrogen to give **4**–**9** is accomplished via either reductive amination or alkylation.

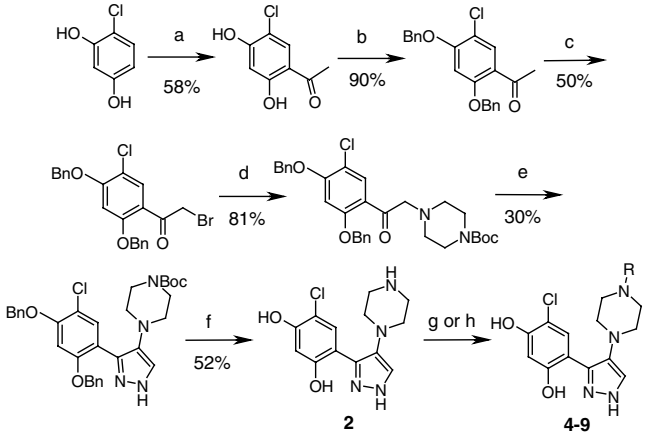

Scheme 1. Synthesis of 3-(5′-chloro)aryl-4-piperazinyl pyrazoles. Reagents and conditions: (a) AcOH, $BF_3{\cdot}OEt_2$, 90 °C, 3.5 h; (b) BnBr, K_2CO_3, MeCN, reflux, 6 h then rt o/n; (c) $PhMe_3N^+Br_3^-$, THF, rt, 2 h; (d) Boc-piperazine, Cs_2CO_3, DMF, rt, 2 h; (e) i—DMF DMA, reflux, 7 h; ii—hydrazine, EtOH, microwave, 120 °C, 5 min; (f) BCl_3, CH_2Cl_2, 0 °C to rt, 1 h; (g) RCHO, $NaBH(OAc)_3$, AcOH, CH_2Cl_2, rt, 3 h; (h) RBr, Cs_2CO_3, DMF, rt, 3 d.

Synthesis of a variety of lipophilic substituents appended to the 5′-position of the resorcinol started from 2,4-dihydroxy acetophenone (Scheme 2). Di-*O*-benzyl protection was followed by selective bromination of the acyl group with phenyltrimethylammonium tribromide. Further bromination with *N*-bromosuccinimide yielded the desired dibromo intermediate which could be elaborated as described in Scheme 1 to furnish **10**. Alkylation of **10** with methylsulfonylbenzyl chloride gave **14**. Pd-catalysed Suzuki coupling to **10** with aryl boronates yielded **12** and Heck coupling with styrene followed by hydrogenation gave **11**. Alkyation of these coupled products proceeded smoothly to give the more complex derivative **14** (Scheme 3).

Exploring the pyrazole 5-position was achieved with a directed lithiation procedure, quenching with a suitable electrophile such as ethyl isocyanate to give ethyl amide **17**. Primary alcohol **16** was prepared by reduction of an intermediary *tert*-butyl ester.

Piperidines **18**–**20** were prepared as for Scheme 1, substituting 4-piperidone for *N*-Boc piperazine in step d. The resulting ketone was reduced to give alcohol **18** and reductively aminated with methylsulfonyl benzylamine and ethylamine to give **19** and **20**, respectively.

N-terminal human Hsp90α his-tagged protein was co-crystallised in complex with compounds **2**, **6** and **17** as previously described.[17] Data were collected on all three co-crystals and the structures subsequently solved by molecular replacement using the previously solved native Hsp90α structure[17] (PDB code: 1UY1). All three co-crystals diffracted in space group I222 to resolutions of 1.8, 2.5 and 2.3 Å for **2**, **6** and **17**, respectively. The previously reported flexible loop region of Hsp90

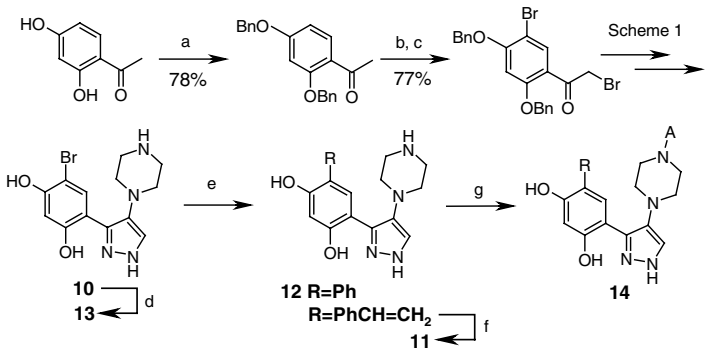

Scheme 2. Synthesis of 5′-analogues of 3-aryl,4-piperazinyl pyrazoles. Reagents and conditions: (a) BnBr, K_2CO_3, MeCN, rt, o/n; (b) $PhMe_3N^+Br_3^-$, THF, rt, 2 h; (c) NBS, DMF, rt, o/n; (d) A-Cl, Cs_2CO_3, DMF, rt, o/n; (e) $ArB(OH)_2$ or $ArCH{=}CH_2$, $PdCl_2[(o\text{-tolyl})_3P)_2$ (2 mol%), $^iPr_2NEt$, *n*BuOH, reflux, 15 h; (f) H_2, 10% Pd/C, EtOAc, rt, 1 h; (g) A-Cl, Et_3N, DMF, rt, o/n.

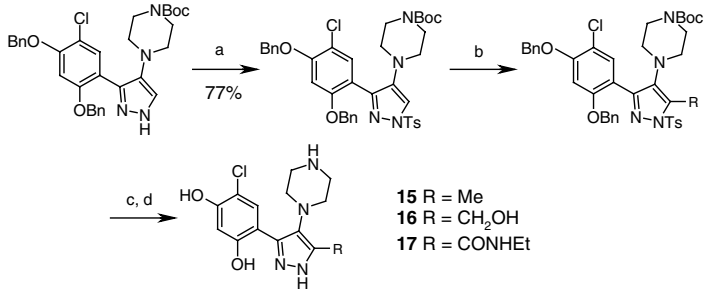

Scheme 3. Synthesis of 5-analogues of 3-aryl,4-piperazinyl pyrazoles. Reagents and conditions: (a) TsCl, pyr, CH_2Cl_2, rt, o/n; (b) i—*n*-BuLi, THF, −78 °C, 10 min; ii—MeI (R = Me) or ^{t}BuOCOCl (R = $CO_2{}^t$Bu) or EtNCO (R = CONHEt), warm to rt; (c) BCl_3, CH_2Cl_2, 0 °C to rt; (d) (R = CH_2OH only) LAH, Et_2O, rt, 2 h.

(residues 108–114) is in a 'closed' conformation[5] in all of these structures. The binding mode of the resorcinol and pyrazole rings is as previously described.[14] All quantum-mechanical calculations were carried out using GAMESS.[19] All molecules in Table 2 were fully minimized, in vacuo and using the PCM model[20] to simulate aqueous solution. In both cases, the minimization started either from the crystallographic structure (*anti*) or a rotation of 180° of the amide (*syn*). The level of calculation was HF/6-31G(d).

To support the fact that the cellular growth inhibition of the more active compounds **2**, **6**, **7** and **13** was through Hsp90 inhibition, the ability of these compounds to modulate the Hsp90 specific cellular markers Raf-1 and Hsp70 was determined. All four compounds down-regulate Raf-1 at doses between 1 and 2 times the cellular GI_{50} level and upregulate Hsp70 (as measured by an Hsp70 specific ELISA) at 1-times the GI_{50} (Fig. 5).

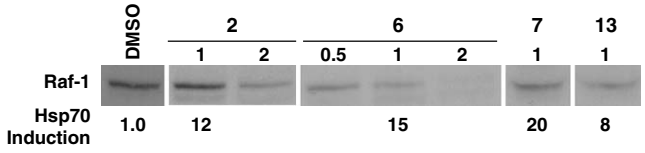

Figure 5. Western blot showing the depletion of Raf-1 levels and induction of Hsp70 (as measured by a Hsp70 specific ELISA) in HCT116 cells following exposure to either 0.5, 1 or 2 times GI_{50} of **2**, **6**, **7** or **13** for 48 h.

These results are in agreement with those seen for the published Hsp90 inhibitors 17-AAG and VER-49009.[11]

In summary, we have discovered novel and soluble 4-amino analogues of the 3-aryl pyrazole series of Hsp90 inhibitors. Crystal structures of the new compounds bound to the enzyme help to explain the observed SAR and suggest further compounds which may be of interest for future studies.

References and notes

1. Jolly, C.; Morimoto, R. I. *J. Natl. Cancer Inst.* **2000**, *92*, 1564.
2. Maloney, A.; Workman, P. *Expert Opin. Biol. Ther.* **2002**, *2*, 3.
3. Workman, P. *Curr. Cancer Drug Targets* **2003**, *3*, 297.
4. Isaacs, J. S.; Xu, W.; Neckers, L. *Cancer Cell* **2003**, *3*, 213.
5. Stebbins, C. E.; Russo, A. A.; Schneider, C.; Rosen, N.; Hartl, F. U.; Pavletich, N. P. *Cell (Cambridge, MA)* **1997**, *89*, 239.
6. Jez, J. M.; Chen, J. H.; Rastelli, G.; Stroud, R. M.; Santi, D. V. *Chem. Biol.* **2003**, *10*, 361.
7. Banjeri, U.; Judson, I.; Workman, P. *Curr. Cancer Drug Targets* **2003**, *3*, 385.
8. Erlichman, C.; Toft, D.; Reid, J.; Sloan, J.; Atherton, P.; Adjei, A.; Ames, M.; Croghan, G. *Proced. Am. Assoc. Cancer Res.* **2001**, *42*, 833.
9. Munster, P. N.; Tong, L.; Schwartz, L.; Larson, S.; Kenneson, K.; De La Cruz, A.; Rosen, N.; Scher, H. *Proced. Am. Soc. Clin. Oncol.* **2001**, *20*, 83a.

10. Yanin, Y. L. *J. Med. Chem.* **2005**, *48*, 7504.
11. Tomura, A.; Odanaka, J.; Takashio, K.; Kuramochi, H. Preparation of pyrazoles as HSp90 inhibitors and their use as antitumor agents. Jpn Kokai Tokkyo Koho JP 2005225787, 2005.
12. Cheung, K.-M.; Matthews, T. P.; James, K.; Rowlands, M. G.; Boxall, K. J.; Sharp, S. Y.; Maloney, A.; Roe, S. M.; Prodromou, C.; Pearl, L. H.; Aherne, G. W.; McDonald, E.; Workman, P. *Bioorg. Med. Chem. Lett.* **2005**, *15*, 3338.
13. Dymock, B. W.; Barril, X.; Brough, P. A.; Cansfield, J. E.; Massey, A.; McDonald, E.; Hubbard, R. E.; Surgenor, A.; Roughley, S. D.; Webb, P.; Workman, P.; Wright, L.; Drysdale, M. J. *J. Med. Chem.* **2005**, *48*, 4212.
14. Kreusch, A.; Han, S.; Brinker, A.; Zhou, V.; Choi, H.-a.; Yun, H.; Lesley, S. A.; Caldwell, J.; Gu, X. J. *Bioorg. Med. Chem. Lett.* **2005**, *15*, 1475.
15. Howes, R.; Barril, X.; Dymock, B. W.; Grant, K.; Northfield, C. J.; Robertson, A. G.; Surgenor, A.; Wayne, J.; Wright, L.; James, K.; Matthews, T.; Cheung, J.; McDonald, E.; Workman, P.; Drysdale, M. J. *Anal Biochem* **2006**, doi:10.1016/j.ab.2005.12.023.
16. The values obtained for the ATPase and the FP assay differ between compounds as they measure different aspects of compound activities. The ATPase assay measures a compound's ability to inhibit ATPase functionality of yeast Hsp90. In comparison, the FP assay measures the ability of a compound to compete with a small molecule for binding to human Hsp90. Therefore, some compounds may compete for binding to Hsp90 with this small molecule poorly due to their kinetic properties (e.g., fast-on, fast-off) but may still retain the ability to inhibit the ATPase activity.
17. Wright, L.; Barril, X.; Dymock, B.; Sheridan, L.; Surgenor, A.; Beswick, M.; Drysdale, M.; Collier, A.; Massey, A.; Davies, N.; Fink, A.; Fromont, C.; Aherne, W.; Boxall, K.; Sharp, S.; Workman, P.; Hubbard, R. E. *Chem. Biol.* **2004**, *11*, 775.
18. Data not shown. Compounds were prepared by alkylation with Cs_2CO_3 and alkyl halide. Regioisomers were separated by preparative HPLC-MS and regiochemistry was determined by NOE spectroscopy.
19. Schmidt, M. W.; Baldridge, K. K.; Boatz, J. A.; Elbert, S. T.; Gordon, M. S.; Jensen, J. J.; Koseki, S.; Matsunaga, N.; Nguyen, K. A.; Su, S.; Windus, T. L.; Dupuis, M.; Montgomery, J. A. *J. Comput. Chem.* **1999**, *14*, 1347.
20. Tomasi, J.; Persico, M. *Chem. Rev.* **1994**, *94*, 2027.
21. Atomic coordinates have been deposited with the Protein Data Bank at Rutgers University (http://rscb.rutgers.edu/pdb/index.html). PDB id codes for **2**, **6** and **17** co-crystallised with Hsp90 are 2CCS, 2CCU and 2CCT, respectively.